eIF3k regulates apoptosis in epithelial cells by releasing caspase 3 from keratin-containing inclusions

Yu-Min Lin[1], Yi-Ru Chen[2], Jia-Ren Lin[3], Won-Jing Wang[2], Akihito Inoko[4], Masaki Inagaki[4], Yi-Chun Wu[5] and Ruey-Hwa Chen[1,2,3,*]

[1]Institute of Biochemical Sciences, National Taiwan University, Taiwan
[2]Institute of Biological Chemistry, Academia Sinica, Taipei, Taiwan
[3]Institute of Molecular Medicine, College of Medicine, National Taiwan University, Taiwan
[4]Division of Biochemistry, Aichi Cancer Center Research Institute, Nagoya 464-8681, Japan
[5]Institute of Molecular and Cellular Biology and Department of Life Science, National Taiwan University, Taiwan
*Author for correspondence (e-mail: rhchen@gate.sinica.edu.tw)

Accepted 30 April 2008
Journal of Cell Science 121, 2382-2393 Published by The Company of Biologists 2008
doi:10.1242/jcs.021394

Summary

Keratins 8 and 18 (collectively referred to as K8/K18) are the major components of intermediate filaments of simple epithelial cells. Recent studies have revealed the function of K8/K18 in apoptosis modulation. Here, we show that eIF3k, originally identified as the smallest subunit of eukaryotic translation initiation factor 3 (eIF3) complexes, also localizes to keratin intermediate filaments and physically associates with K18 in epithelial cells. Upon induction of apoptosis, eIF3k colocalizes with K8/K18 in the insoluble cytoplasmic inclusions. Depletion of endogenous eIF3k de-sensitizes simple epithelial cells to various types of apoptosis through a K8/K18-dependent mechanism and promotes the retention of active caspase 3 in cytoplasmic inclusions by increasing its binding to keratins. Consequently, the cleavage of caspase cytosolic and nuclear substrates, such as ICAD and PARP, respectively, is reduced in eIF3k-depleted cells. This study not only reveals the existence of eIF3k in a subcellular compartment other than the eIF3 complex, but also identifies an apoptosis-promoting function of eIF3k in simple epithelial cells by relieving the caspase-sequestration effect of K8/K18, thereby increasing the availability of caspases to their non-keratin-residing substrates.

Supplementary material available online at
http://jcs.biologists.org/cgi/content/full/121/14/2382/DC1

Key words: Keratin 8, Keratin 18, Caspase compartmentalization, Apoptosis, eIF3k

Introduction

Eukaryotic translation initiation factor 3 (eIF3) plays essential roles in translational initiation (Hinnebusch, 2006). The mammalian eIF3 complex consists of 10-13 non-identical subunits, including five highly conserved core subunits and five to eight less-conserved non-core subunits (Phan et al., 1998; Browning et al., 2001). The 28 kDa eIF3k protein was identified as a subunit of the eIF3 complex by its co-purification with the entire complex and by its direct association with several eIF3 subunits (Burks et al., 2001; Mayeur et al., 2003). Structural analysis reveals that eIF3k consists of a HEAT-repeat-like HAM domain and a winged-helix-like WH domain, suggesting a role of eIF3k in protein-protein and protein-RNA interactions (Wei et al., 2004). It is currently unknown whether eIF3k contributes to or regulates the activity of the eIF3 complex in translational initiation in vivo. However, recent reconstitution analysis revealed that this non-core subunit is dispensable for the formation of active eIF3 complex in vitro (Masutani et al., 2007). eIF3k has been reported to interact with cyclin D3 (Shen et al., 2004) and with 5-HT(7) receptor (De Martelaere et al., 2007), implicating its involvement in translation-unrelated biological processes.

Keratin intermediate filaments are preferentially expressed in epithelial cells and epidermal appendages. Keratins exist as heteropolymers composed of type I (K9-K20) and type II (K1-K8) subunits (Coulombe and Omary, 2002; Porter and Lane, 2003). Keratin 8 and keratin 18 (collectively K8/K18) are major components of the intermediate filaments of simple or single-layered epithelium. One important function of keratin filaments is to provide mechanical strength to cells, thereby protecting them from mechanical injury. However, emerging evidence has revealed the non-mechanical functions of keratins, such as modulation of signal transduction pathways, susceptibility to apoptosis, protein subcellular targeting and organelle transport (Coulombe and Omary, 2002; Oshima, 2002; Toivola et al., 2005; Betz et al., 2006; Kim and Coulombe, 2007; Magin et al., 2007). A number of studies have demonstrated the function of keratins in modulating apoptosis. For instance, epithelial cells or hepatocytes deficient in K8 and/or K18 are more sensitive to apoptosis induced by TNFα or Fas ligation than their control counterparts (Caulin et al., 2000; Gilbert et al., 2001). A similar role of K17 in modulating the TNFα pathway, thereby participating in the involution phase of hair-follicle recycling, was revealed with K17-null mice (Tong and Coulombe, 2006). Interestingly, keratins seem to antagonize death-receptor pathways through multiple mechanisms. First, K8-null hepatocytes display an increased targeting of Fas to the cell surface (Gilbert et al., 2001). Second, K18 and K17 bind and sequester TRADD, an adaptor protein that is recruited to the TNFRI and is essential for downstream signal relay (Inada et al., 2001). Finally, K8 can

compete with non-keratin pro-apoptotic substrates for phosphorylation by stress-activated kinase, and expression of a phosphorylation-defective K8 mutant enhances Fas-mediated apoptosis in transgenic mouse livers (Ku and Omary, 2006). This suggests that the highly abundant K8 might serve as a 'phosphate sponge' to prevent cell death and tissue injury under various stress conditions.

In addition to modulating death-receptor-mediated apoptosis, keratins have a more general effect in apoptosis, controlling key stages of the caspase activation cascade. In epithelial cells receiving death stimuli that activates either the death-receptor or mitochondrial-dependent pathway, the death effector domain-containing DNA binding protein (DEDD) directs procaspase 3 to keratin filaments at an early stage of apoptosis, preceding caspase activation and nuclear changes (Lee et al., 2002). Furthermore, the catalytically active caspase 9, cleaved at both Asp315 and Asp330, is similarly concentrated on keratin fibrils (Dinsdale et al., 2004). Emerging evidence supports a model in which keratin filaments and their associated DEDD provide a scaffold for accumulation and auto-activation of procaspase 9, which in turn cleaves procaspase 3 that is within close proximity. The active caspase 3 can further activate procaspase 9 through cleavage at Asp330, thereby facilitating a caspase amplification loop (Dinsdale et al., 2004). In line with this model, knockdown of DEDD or expression of its keratin-targeting-defective mutant inhibits activation of caspase 3 (Lee et al., 2002). Furthermore, the capability of DEDD to associate with K8/K18 filaments correlates strongly with heightened sensitivity to apoptosis in many epithelial cells (Schutte et al., 2006). Thus, the keratin network nucleates apoptotic machinery and confers a caspase-activation and/or -amplification platform. In the meantime, K18 is cleaved by effector caspases, leading to the collapse of K8/K18 filaments to form punctate inclusions (Ku et al., 1997; Ku and Omary, 1997; Leers et al., 1999; Oshima, 2002; Schutte et al., 2004). These cytoplasmic inclusions contain not only K8 and caspase-cleaved K18, but also several pro-apoptotic factors, such as active caspase 9 and caspase 3, DEDD, and TRADD, and thus might function as sequestosomes to reduce the availability of caspases to their substrates (Dinsdale et al., 2004). As the apoptosis program proceeds, it is currently unclear whether and how a portion of active caspases can be released from these inclusions to facilitate the cleavage of other cellular substrates.

Here, we identify a novel subcellular localization and biological function of eIF3k. We found that a large portion of cellular eIF3k colocalizes with K8/K18 filaments in non-apoptotic cells and with K8/K18-containing inclusions in apoptotic cells. Endogenous eIF3k sensitizes K8/K18-containing cells to apoptosis induced by various agents, but does not elicit any death-regulating effect on keratin-deficient cells. Furthermore, we provide evidence showing that eIF3k regulates apoptosis by promoting the release of active caspase 3 from the insoluble cytoplasmic inclusions.

Results

Characterization of the eIF3k antiserum

To characterize the eIF3k protein, we generated polyclonal antiserum against human eIF3k. Whereas pre-immune serum did not recognize any protein in the cell lysate (data not shown), the eIF3k antiserum recognized both bacterially expressed GST-eIF3k and a unique protein migrating at 28 kDa in HeLa cells (Fig. 1A). The size of this protein is in agreement with the calculated molecular weight of eIF3k. This antiserum also reacted with FLAG-tagged eIF3k in lysate of transfected cells (Fig. 1A). To

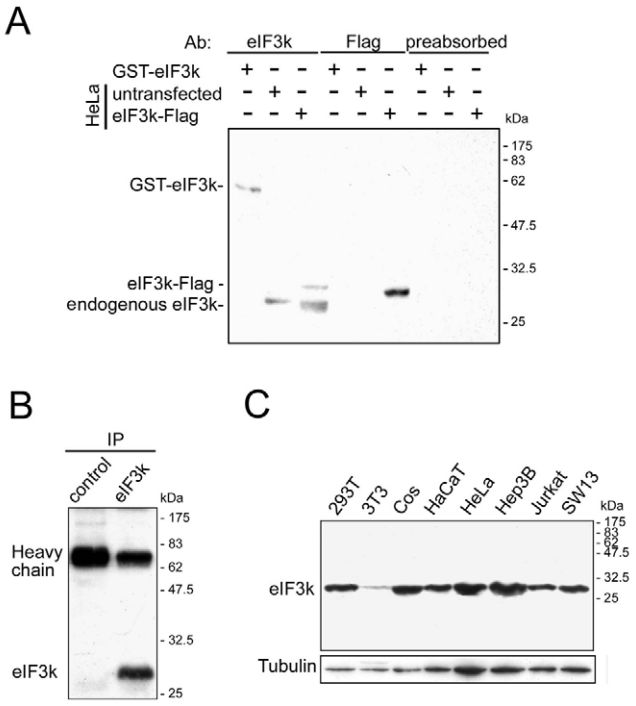

Fig. 1. Characterization of the eIF3k antiserum. (A) Western blot analyses on lysates from untransfected HeLa cells or HeLa cells transfected with FLAG-tagged eIF3k (eIF3k-Flag), or on GST-eIF3k purified from bacteria (GST-eIF3k). Antibodies used are eIF3k antiserum, anti-Flag and eIF3k antiserum pre-absorbed with GST-eIF3k. (B) Immunoprecipitation analysis with the eIF3k antiserum or a control antiserum. Lysates of HEK 293T cells were used for immunoprecipitations with antibodies as indicated, followed by western blot with eIF3k antiserum. (C) Expression of eIF3k in various cells as indicated. All cell lines are from human origin except for NIH3T3 (3T3) and Cos-1 (Cos).

demonstrate the specificity of the antiserum, GST-eIF3k bound on beads was used to deplete the anti-eIF3k antibodies. The pre-absorbed antiserum failed to react with any protein in cell lysate (Fig. 1A). When the eIF3k antiserum was employed for immunoprecipitation, we observed a specific precipitation of endogenous eIF3k from cell lysate (Fig. 1B). Together, these data indicate that the antiserum is capable of specifically recognizing eIF3k in both immunoblot and immunoprecipitation analyses. With this antiserum, we found that the 28 kDa eIF3k protein is expressed in a variety of cell types (Fig. 1C).

eIF3k colocalizes with K8/K18 filaments

Next, we determined the subcellular localization of eIF3k. Surprisingly, immunostaining analyses with the eIF3k antiserum revealed a filamentous pattern of endogenous eIF3k in both HeLa and HaCaT epithelial cells (Fig. 2A). These filaments displayed a remarkable colocalization with K8/K18 intermediate filaments. Endogenous eIF3k, however, showed no apparent co-distribution with F-actin and microtubules (Fig. 2B). The filamentous distribution of eIF3k was not observed in the keratin-deficient adenocarcinoma cell line SW13 (Hedberg and Chen, 1986) or in NIH3T3 fibroblasts. Instead, eIF3k distributed diffusely in the cytoplasm of these cells (Fig. 2C). To validate the specificity of our immunostaining analysis on eIF3k, we carried out two sets of experiments. In the first set, we absorbed the anti-eIF3k antiserum

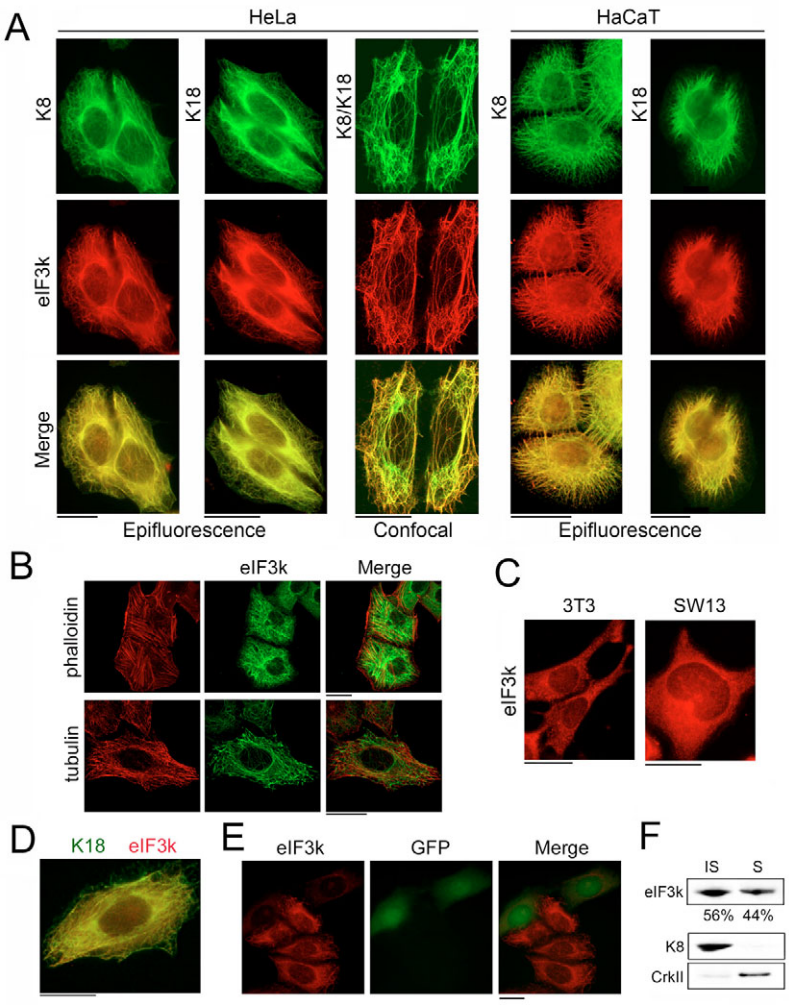

Fig. 2. Characterization of the subcellular distribution of eIF3k. (A) eIF3k colocalizes with K8 and K18. HeLa and HaCaT epithelial cells were fixed, double stained with anti-eIF3k antiserum and antibody to K8 or K18, and examined by epifluorescence or confocal microscopy as indicated. One confocal section corresponding to each individual labeling is shown. The overlay of green and red images is shown in the 'Merge' panel. (B) eIF3k does not colocalize with F-actin or microtubules. HeLa cells were fixed, double stained with eIF3k antiserum and either rhodamine-phalloidin or anti-α-tubulin, and examined by confocal microscopy.
(C) Immunofluorescence analysis of eIF3k distribution in cells without keratin filaments. SW13 and NIH3T3 cells were immunostained with the eIF3k antiserum and then examined by epifluorescence microscopy. (D) The eIF3k antiserum does not crossreact with an epitope in K18. The eIF3k antiserum was pre-absorbed with 100 μg recombinant K18. HeLa cells were double stained by the pre-absorbed eIF3k antiserum (red) and anti-K18 antibody (green), and were examined by epifluorescence microscopy. (E) HeLa cells stably expressing *eIF3k* siRNA and GFP (see Fig. 5A for description) were mixed with parental HeLa cells and then examined by immunostaining with eIF3k antiserum. (F) Distribution of eIF3k in both the detergent-soluble and -insoluble compartments of cells. HeLa cells were extracted with lysis buffer containing 0.5 % Triton X-100 (see Materials and Methods). The detergent-soluble and -insoluble fractions were collected and one fifteenth of each fraction was separated by SDS-PAGE followed by western blot analyses with antibodies as indicated. CrkII and K8 were used as the reference protein for soluble and insoluble fractions, respectively. The percentages indicate the amount of eIF3k in each fraction. Scale bars: 5 μm.

with recombinant K18 to rule out the possibility that eIF3k and K18 share certain cryptic epitopes. Importantly, the resulting antiserum could still confer a K18-colocalization pattern in the immunostaining analysis (Fig. 2D). As a control, the same amount of recombinant K18 almost completely depleted the anti-K18 antibody, as revealed by the drastically reduced signal in the immunostaining analysis (see Fig. S1 in supplementary material). In the second set of experiments, we generated HeLa cells stably expressing *eIF3k*-specific siRNA and GFP (see Fig. 5A for a description). The stable transfectants were mixed with parental HeLa cells and examined by immunostaining with the eIF3k antiserum. Notably, cells carrying *eIF3k* siRNA, as visualized by their GFP fluorescence, displayed a much weaker staining with the eIF3k antiserum, compared with untransfected cells (Fig. 2E). Together, these results strongly demonstrate the specificity of our immunostaining data. Because the fixation procedure used in these immunofluorescence analyses might lead to a loss of certain soluble proteins, we employed a biochemical analysis to investigate whether eIF3k could also be found in the cytosol, in which the eIF3 complex resides. To this end, HeLa cells were extracted with Triton X-100 to separate the soluble proteins from the insoluble cytoskeleton. As expected, K8 was found exclusively in the detergent-insoluble fraction. Approximately 56% of the total eIF3k was cofractionated with K8, whereas the rest was present in the detergent-soluble compartment (Fig. 2F). Thus, these immunostaining and biochemical data indicate that eIF3k can be recruited to at least two subcellular compartments.

Next, we examined whether the colocalization of eIF3k with K8/K18 could be recapitulated in mouse tissues. Immunofluorescence analysis on stomach sections revealed the enrichment of both K8 and eIF3k in the luminal surface of glandular-stomach mucosa. This concentration of eIF3k and K8 at the apical region of epithelial cells was also observed in prostate epithelium and intestine enterocytes (Fig. 3). In addition, partial colocalization of eIF3k with K8 was revealed in the cell-cell border of enterocytes (Fig. 3, bottom panel) and prostate epithelial cells as well as in goblet cells of the intestine. Consistent with its ubiquitously expressing nature, eIF3k expression could also be found in lamina propria of the intestine, in which K8 expression was absent. Together, these results indicate the colocalization of eIF3k with K8 in mouse tissues.

eIF3k associates with K18

The colocalization of eIF3k with K8/K18 filaments prompted us to investigate the possible interaction between eIF3k and K8 or K18. Yeast two-hybrid analysis revealed that Gal4-eIF3k interacted with LexA-K18 but not with LexA-K8. As controls, Gal4-eIF3k did not interact with LexA-lamin, nor did LexA-K8 or LexA-K18 bind Gal4 alone (Fig. 4A). We next examined the interaction of endogenous eIF3k with endogenous K18 in mammalian cells. HeLa cells were

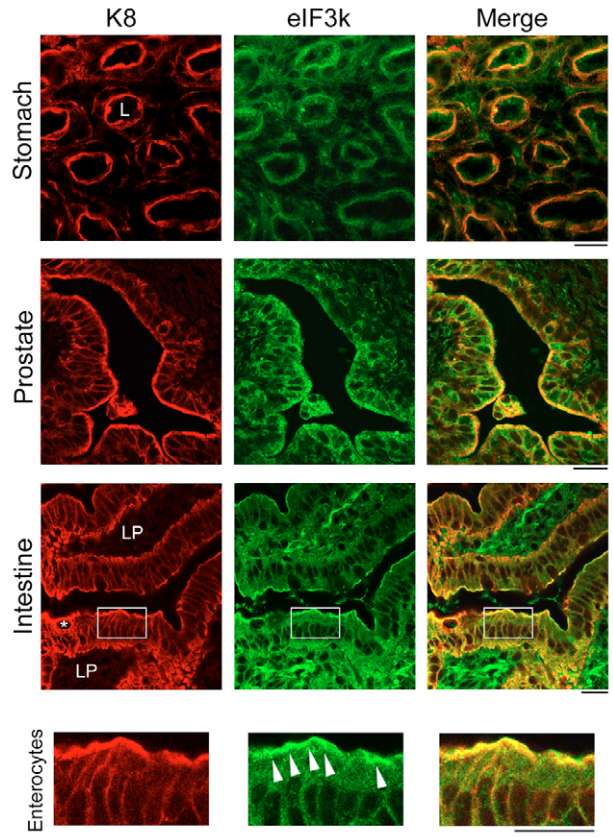

Fig. 3. Distributions of eIF3k and K8 in various tissues. Sections of indicated mouse tissues were double stained with anti-eIF3k and -K8 antibody (Troma-1), and then analyzed by confocal microscopy. Boxed regions are magnified in the bottom panel. The asterisk indicates a goblet cell. The concentration of staining at the apical pole of the enterocytes is marked by arrowheads. L, lumen; LP, lamina propria. Scale bars: 25 μm.

extracted with the detergent Empigen BB, which is reported to solubilize ~40% of cellular keratins in epithelial cell lines, yet preserve the complex formed by keratins and their interacting proteins (Lowthert et al., 1995). Immunoprecipitation analysis using Empigen-BB-solubilized cell lysates and anti-K8/K18 antibodies revealed a co-precipitation of eIF3k (Fig. 4B, upper panel). Reciprocally, immunoprecipitation with the eIF3k antiserum co-precipitated K18 (Fig. 4B, lower panel). Quantitation analysis indicated that a significant portion (16.5±6.4%) of total cellular eIF3k was associated with K18 in vivo (see Fig. S2 in supplementary material).

To map the regions in eIF3k and K18 that are responsible for their interaction, we generated a series of truncation mutants of these two proteins. Yeast two-hybrid analyses demonstrated that the HAM domain, but not the WH domain, was capable of interacting with K18 (Fig. 4C). In addition, K18 constructs containing the head domain could bind eIF3k (Fig. 4D). These results indicate that the eIF3k HAM domain interacts with the K18 head domain.

Downregulation of eIF3k attenuates apoptosis

The colocalization of eIF3k with K8/K18 filaments and its association with K18 prompted us to investigate a possible role of

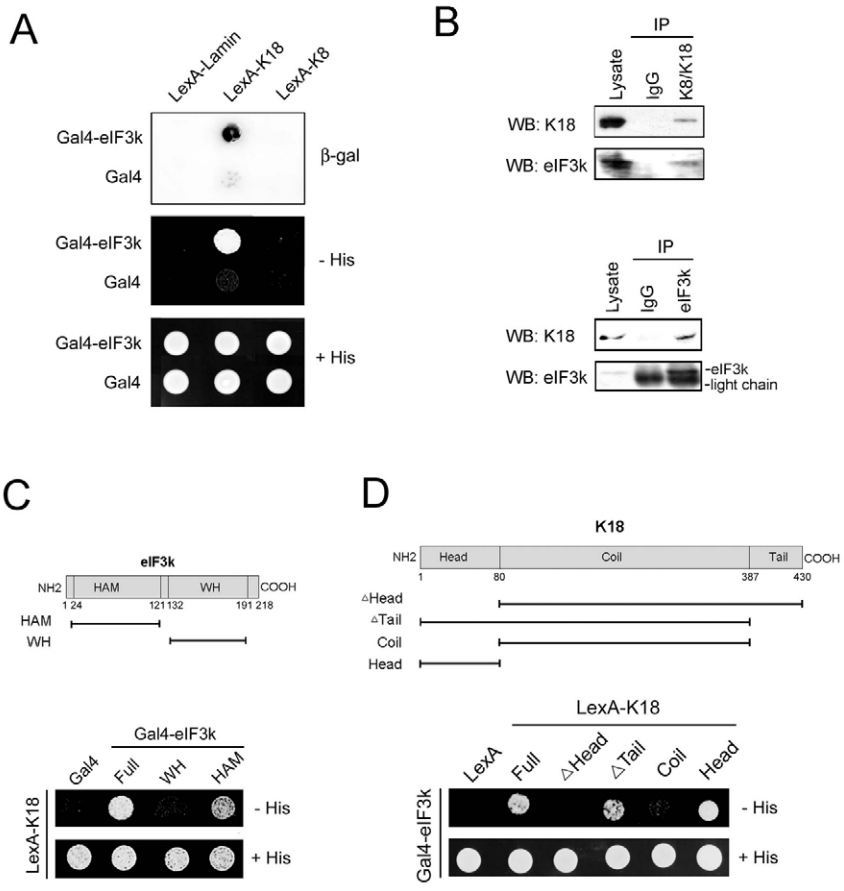

Fig. 4. Interaction of eIF3k with K18. (A) Yeast two-hybrid assay. Yeast strain L40 was co-transformed with LexA- and Gal4-based vectors as indicated. The transformants were tested for β-galactosidase activity (β-gal; upper panel) and for their ability to grow in medium without histidine (middle panel) as described in the Materials and Methods. Yeast grown on the –His plate and that stained positive for β-galactosidase activity indicate the interaction between proteins encoded by the two plasmids. (B) eIF3k interacts with K18 endogenously. HeLa cells were lysed with Empigen BB lysis buffer as described in the Materials and Methods, and then subjected to immunoprecipitations with antibodies to K8 and K18 (1:1 mixture of anti-K8 and -K18 antibodies; upper panel), eIF3k (lower panel) or a control IgG (both panels). The immunoprecipitates and cell lysates were resolved by SDS-PAGE and then analyzed by western blot with antibodies as indicated. The positions of immunoglobulin light chain and eIF3k are indicated in the bottom panel. (C,D) Mapping of the domains in eIF3k (C) and K18 (D) that are responsible for their interaction. Yeast strain L40 was transformed with LexA- and Gal4-based vectors as indicated and analyzed as in A. Domain organizations of eIF3k, K18 and mutants used in this study are shown in the top panel. Numbers refer to amino acid positions.

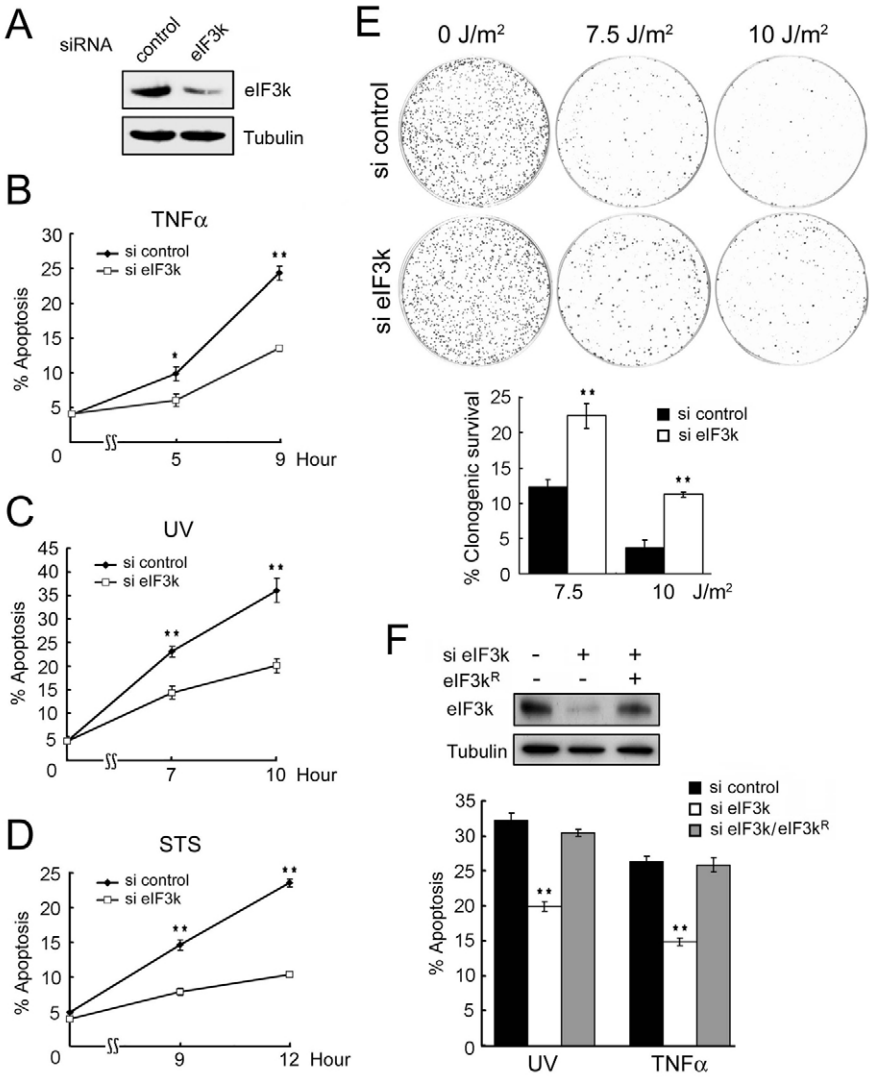

Fig. 5. Downregulation of eIF3k protects cells from apoptosis. (A) Generation of *eIF3k* siRNA stable transfectants. HeLa cells were co-transfected with plasmid expressing *eIF3k*-specific siRNA or control siRNA and the plasmid pEGFP/Neo^r (carrying both GFP and the neomycin-resistant gene) at a ratio of 4:1. Cells were selected with G418. For transfectants carrying the control vector, all G418-resistant clones were pooled. *eIF3k*-siRNA transfectants were first tested for the expression of eIF3k and seven clones displaying a reduced level of eIF3k were pooled. The two pools of stable transfectants were lysed and subjected to western blot with antibodies to eIF3k and tubulin. (B-D) HeLa cells stably expressing *eIF3k* siRNA or control siRNA as described in A were assayed for apoptosis by flow-cytometry analysis of cells with fragmented DNA (sub-G1 DNA). The percentage of cells with fragmented DNA is plotted. In B and D, cells were treated with 10 ng/ml TNFα together with 2.5 ng/ml Actinomycin D (B) or 1 μM staurosporine (STS, D), respectively, for various durations. In C, cells were irradiated with UV at 0.015 J/cm^2 and then cultured for various durations as indicated. (E) Clonogenic survival of UV-irradiated cells carrying *eIF3k* siRNA or control siRNA. HeLa cells as in A were irradiated with UV at the indicated doses. Cells were cultured for 8 days and then stained by crystal violet. Colony numbers were quantitated by ImageJ software. The percentage of clonogenic survival was determined by the ratio of colony numbers derived from the treated population to those from the untreated population. (F) Expression of the siRNA-resistant *eIF3k* (eIF3k^R) construct reverses the apoptosis-modulating effect of *eIF3k* siRNA. HeLa cells transfected with constructs as indicated were assayed for apoptosis induced by UV or TNFα (bottom panel), or the level of eIF3k (upper panel). For B-F, data shown are mean ± s.d. from three independent experiments. **P*<0.05; ***P*<0.005.

eIF3k in keratin-filament organization or in cellular functions related to keratins. Neither overexpression nor knockdown of eIF3k in HeLa cells caused a detectable alteration in K8/K18-filament organization as shown by immunostaining analysis (Fig. S3A,B in supplementary material). Because recent studies have demonstrated an involvement of K8/K18 and their associated proteins in apoptosis modulation (Coulombe and Omary, 2002; Oshima, 2002; Toivola et al., 2005; Kim and Coulombe, 2007), we explored the influence of eIF3k on the susceptibility of epithelial cells to apoptosis. To this end, HeLa cells were transfected with constructs expressing *eIF3k*-specific siRNA or control siRNA together with pEGFP-Neo^r. After selection with G418, a pool of stable transfectants carrying either siRNA was generated. In the pool of cells expressing *eIF3k* siRNA, the level of endogenous eIF3k was markedly reduced compared with cells carrying control siRNA (Fig. 5A). When these two populations of cells were treated with TNFα, the pool of *eIF3k*-siRNA-expressing cells displayed a reduced sensitivity to apoptosis, compared with cells carrying control siRNA (Fig. 5B). Thus, in contrast to the protective effect of K8/K18 on TNFα-induced apoptosis (Caulin et al., 2000), our data demonstrated an apoptosis-promoting function of the keratin-residing eIF3k. To determine whether this function of eIF3k is restricted to the death-receptor axis, we treated cells with UV or staurosporine, both of which activate the mitochondrial-dependent apoptotic pathway. Similarly, knockdown of eIF3k led to significant protection against apoptosis induced by UV or staurosporine (Fig. 5C,D). This protection against cell death following eIF3k depletion was reflected in terms of long-term survival because it was found to cause a considerable increase in the clonogenic survival of UV-irradiated cells (Fig. 5E). Of note, this increase of clonogenic survival cannot be attributed to an effect of eIF3k on cell growth or protein synthesis, because the two populations of cells displayed similar rates of DNA synthesis and de novo protein synthesis (see Fig. S4A,B in supplementary material). Finally, to demonstrate that the apoptosis-modulating effect is specific to eIF3k downregulation, we generated an siRNA-resistant *eIF3k* construct. Introducing this construct to the eIF3k-knockdown cells not only rescued the level of eIF3k, but also completely reversed the effect of *eIF3k* siRNA on protection against apoptosis (Fig. 5F). Together, these results demonstrate a broad involvement of eIF3k in apoptosis regulation in simple epithelial cells and suggest that eIF3k affects a step shared by both intrinsic and extrinsic apoptosis pathways.

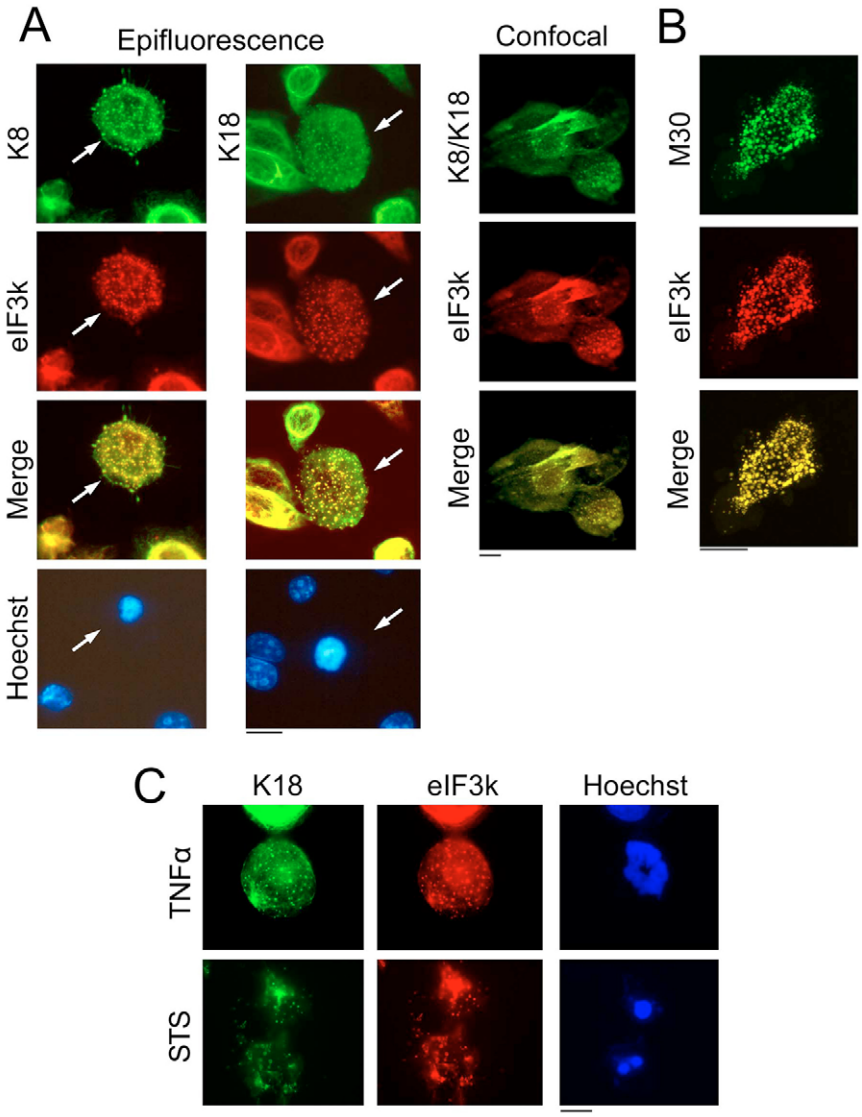

Fig. 6. Colocalization of eIF3k and K8/K18 in cytoplasmic inclusions of apoptotic cells. (A) HeLa cells were irradiated with UV at 0.015 J/cm^2 and then cultured for 7 hours. Cells were fixed, triple stained with Hoechst 33258 and antibodies to eIF3k and K8 or K18, and then examined by epifluorescence or confocal microscopy as indicated. One confocal section corresponding to each individual labeling is shown. The overlay of green and red images is shown in the 'Merge' panel. Apoptotic cells are marked by arrows. (B) Cells as in A were double stained with antibody to eIF3k and with M30, and were examined by confocal microscopy. (C) HeLa cells were treated with 10 ng/ml of TNFα together with 2.5 ng/ml of Actinomycin D for 5 hours, or 1 μM staurosporine for 7 hours. Cells were stained as in A and examined by epifluorescence microscopy. Scale bars: 5 μm.

eIF3k colocalizes with K8/K18 in the cytoplasmic inclusions in apoptotic cells

Having identified the function of eIF3k in apoptosis regulation, we next investigated whether this effect is related to its localization on the keratin network. Because K8/K18 filaments are disrupted to form cytoplasmic inclusions during apoptosis (Oshima, 2002), we first tested whether eIF3k could be found in these inclusions in apoptotic cells. UV-irradiated HeLa cells were examined by double immunostaining with antibodies against eIF3k and K8 or K18. In apoptotic cells, characterized by their condensed nuclei, eIF3k displayed cytoplasmic granule structures and showed a remarkable colocalization with K8 and K18 (Fig. 6A). The existence of eIF3k in keratin-containing cytoplasmic inclusions was further confirmed by immunostaining with the inclusion-body marker M30 (Fig. 6B), which is the antibody recognizing a neoepitope on caspase-3-cleaved K18 (Leers et al., 1999). As expected, inhibition of caspase activity restored the filamentous patterns of both K8/K18 and eIF3k (see Fig. S5 in supplementary material). To determine the generality of localization of eIF3k in cytoplasmic inclusions in apoptotic cells, we evaluated TNFα- and staurosporine-treated cells. Colocalization of eIF3k with K18 in granule structures was also observed in these apoptotic systems (Fig. 6C). Thus, our results indicate that eIF3k colocalizes with K8/K18 in both non-apoptotic and apoptotic cells. In addition, the stoichiometry of eIF3k association with K8/K18 was not altered during apoptosis (data not shown).

K8/K18 are required for the apoptosis-promoting function of eIF3k

Next, we determined whether the apoptosis-regulating effect of eIF3k is related to its colocalization with K8/K18. To this end, we used the EBNA-SW13 cell system, which was developed to study the role of K8/K18 in apoptosis (Inada et al., 2001). This keratin-deficient SW13 cell stably expresses the Epstein-Barr virus (EBV) EBNA-1 protein, thus allowing an efficient re-expression of K8 and K18. First, we introduced *eIF3k* siRNA or control siRNA into the EBNA-SW13 cells and generated pools of stable transfectants. As shown in Fig. 7A, eIF3k expression was significantly reduced in the pool carrying *eIF3k* siRNA, compared with that expressing control siRNA. Next, we evaluated the sensitivities of the two pools of cells to various apoptotic stimuli. Unlike what was observed in HeLa cells, downregulation of eIF3k in keratin-deficient SW13 cells did not affect apoptosis induced by TNFα, UV or staurosporine (Fig. 7B-

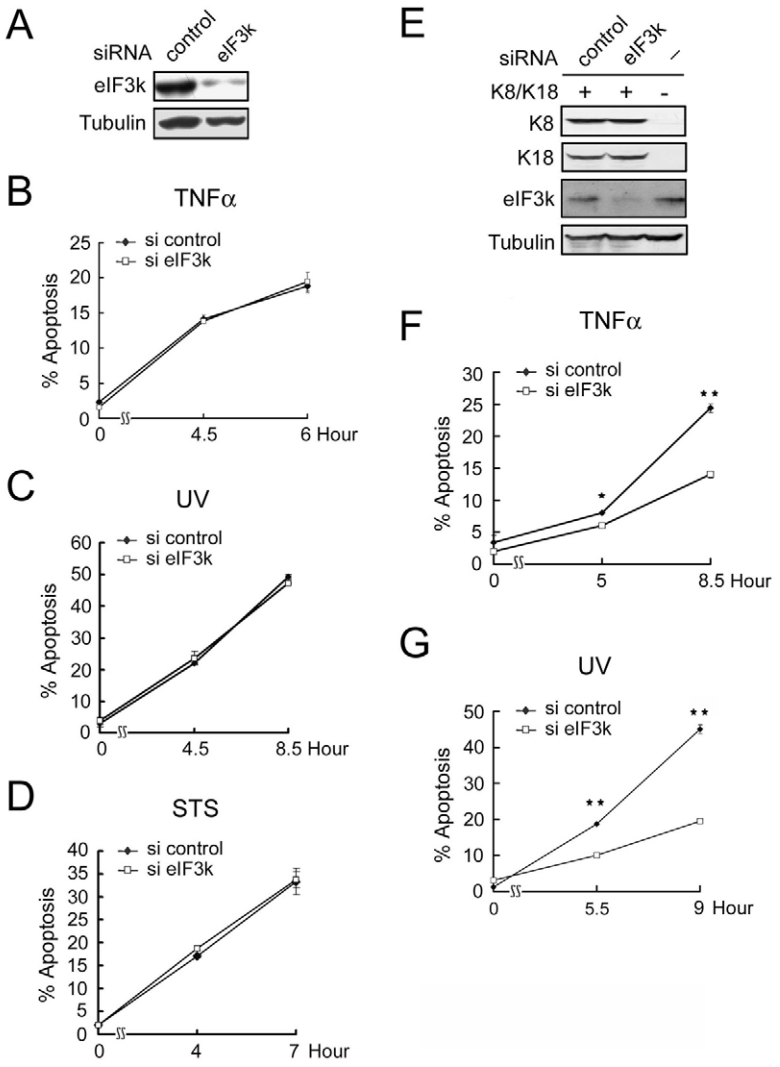

Fig. 7. eIF3k regulates apoptosis in a K8/K18-dependent manner. (A) Generation of *eIF3k*-siRNA stable transfectants. EBNA-SW13 cells were co-transfected with a plasmid expressing *eIF3k* siRNA or control siRNA and a plasmid carrying the puromycin-resistant gene, and then selected with puromycin. Pools of stable transfectants were established as described in Fig. 5 and then used to analyze the expression of eIF3k by western blot. (B-D) Pools of stable transfectants as described in A were treated with 10 ng/ml TNFα together with 2.5 ng/ml Actinomycin D (B), or 1 μM staurosporine (D) for various durations, as indicated. Alternatively, cells were irradiated with UV at 0.015 J/cm^2 and then cultured for the indicated durations (C). (E) EBNA-SW13 cells carrying *eIF3k* siRNA or control siRNA as shown in A were co-transfected with pDR2-K8 and pDR2-K18. The transfectants were selected by hygromycin and then lysed for western blot analysis with antibodies as indicated. Lysate of the parental EBNA-SW13 cells was included to reveal the lack of K8/K18 expression in this cell line. (F,G) SW13-K8/K18 cells carrying *eIF3k* siRNA or control siRNA as shown in E were treated with 10 ng/ml TNFα together with 2.5 ng/ml Actinomycin D (F) or 1 μM staurosporine (G) for various durations as indicated. Apoptotic cells were analyzed as in Fig. 5. Data shown are mean ± s.d. from three independent experiments. **P*<0.05; ***P*<0.005.

D). To further demonstrate the crucial role of K8/K18 in the apoptosis-promoting function of eIF3k, EBNA-SW13 cells carrying *eIF3k* siRNA or control siRNA were co-transfected with pDR2 vectors containing K8/K18 (Inada et al., 2001). These vectors possess the EBV origin of replication and therefore allow high-copy episomal replication in cells expressing EBNA-1. After selection with hygromycin, cells re-expressing both K8/K18 were established (Fig. 7E). Notably, this reintroduction of K8/K18 did not interfere with the efficacy of *eIF3k* siRNA. When the two populations of K8/K18-expressing SW13 cells (SW13-K8/K18 cells) were treated with TNFα (Fig. 7F) or UV (Fig. 7G), cells expressing *eIF3k* siRNA were more resistant to apoptosis than those with control siRNA. Together, our data indicate that the apoptosis-enhancing activity of eIF3k requires the existence of K8/K18 proteins.

eIF3k promotes the release of active caspase 3 from K8/K18-residing insoluble inclusions

The finding that eIF3k affects apoptosis only in cells containing K8/K18, combined with its association with K8/K18, raises the possibility that K8/K18 might mediate the apoptosis-promoting function of eIF3k. Considering the broad involvement of eIF3k in several apoptotic systems in epithelial cells and the previously reported effect of K8/K18 on apoptosis modulation by sequestrating certain apoptotic factors, including active caspases (Lee et al., 2002; Dinsdale et al., 2004), we hypothesized that eIF3k might interfere with the caspase-sequestration capability of K8/K18. To test this possibility, we first assessed the influence of eIF3k on distributions of caspases in the detergent-soluble and detergent-insoluble fractions of apoptotic cells. SW13-K8/K18 cells carrying *eIF3k* siRNA or control siRNA were UV irradiated and then extracted with detergent. Similar to what was observed in HeLa cells (Fig. 2F), K8 existed almost exclusively in the insoluble fraction. Importantly, upon induction of apoptosis, a higher level of active caspase 3 was present in the insoluble fraction in cells expressing *eIF3k* siRNA, compared with those carrying control siRNA (Fig. 8A, upper panel). This increased recruitment of active caspase 3 to the insoluble compartment by *eIF3k* siRNA was accompanied by a concomitant decrease of its content in the soluble fraction. The distribution of procaspase 3, however, was not significantly affected by *eIF3k* siRNA. In addition to SW13-K8/K18 cells, a similar *eIF3k*-siRNA-triggered sequestration of active caspase 3 in the insoluble compartment was observed in HeLa cells (data not shown). Thus, our results demonstrated that endogenous eIF3k promotes a mobilization of active caspases 3 from the insoluble fraction to the soluble cytosol. To further elucidate that the *eIF3k*-induced release of active caspase 3 to the soluble fraction is dependent on the

presence of K8/K18, we assessed the partitions of this caspase 3 into the two fractions in keratin-deficient SW13 cells. Importantly, the distribution of active caspase 3 was not affected by *eIF3k* siRNA (Fig. 8B). Thus, our findings indicate that endogenous eIF3k promotes the release of active caspase 3 from the insoluble compartment via a K8/K18-dependent manner.

Proteins residing in several different subcellular compartments can be fractionated into a Triton-X-100-insoluble fraction. To more precisely determine the influence of eIF3k on caspase distribution and its relevance to K8/K18, we carried out immunostaining analysis. Similar to that shown in Fig. 6, UV irradiation of HeLa cells carrying control siRNA led to the breakdown of K8/K18 filaments to form numerous cytoplasmic inclusions, as detected by the antibody M30. Active caspase 3 displayed both diffused and punctate patterns, and the latter was partially colocalized with M30-positive granules (Fig. 9A and Movies 1, 2 in supplementary material). Remarkably, we observed a significantly enhanced retention of active caspase 3 in M30-positive granules in *eIF3k*-siRNA-expressing cells compared with control-siRNA-expressing cells (Fig. 9A). Quantitative analyses revealed that downregulation of eIF3k resulted in a stronger correlation of the active-caspase-3 image with the M30 image (Fig. 9B) and a higher percentage of M30-positive inclusions containing active caspase 3 (Fig. 9C). Thus, our immunostaining and biochemical analyses provide strong evidence for the role of eIF3k in relieving the caspase-sequestration function of K8/K18.

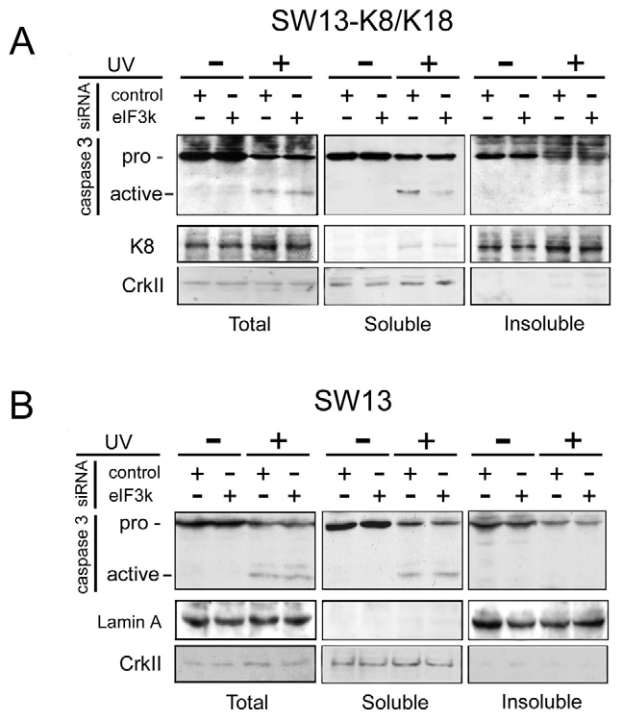

Fig. 8. Knockdown of eIF3k promotes keratin-dependent sequestration of active caspase 3 in the insoluble compartment of cells. SW13-K8/K18 (A) or SW13 (B) cells stably expressing *eIF3k* siRNA or control siRNA as described in Fig. 7E and Fig. 7A, respectively, were irradiated with or without UV at 0.015 J/cm^2 and then cultivated for 7 hours. Cells were extracted with lysis buffer containing 0.5% Triton X-100, and soluble and insoluble fractions were separately collected as described in the Materials and Methods. Equal volumes of the soluble and insoluble fractions were mixed as the total lysates (Total). One fifteenth of each fraction and total lysates were resolved by SDS-PAGE and then analyzed by western blot with antibodies as indicated. CrkII and K8 (or Lamin A) were used as the reference protein for soluble and insoluble fractions, respectively.

eIF3k decreases K8/K18-associated caspase 3 and increases availability of caspase 3 to non-keratin-residing substrates

To investigate the mechanism by which the active caspase is sequestered in K8/K18-positive inductions, we tested whether active caspase 3 could physically interact with K8/K18. GST-pull-down analysis revealed a specific interaction between active caspase 3 and full-length K18, and this interaction was abrogated by deletion of the K18 head domain (Fig. 9D). Because the K18 head domain is also involved in the interaction with eIF3k, we explored a possibility that eIF3k and active caspase 3 compete for binding of K18. Using lysates of UV-irradiated HeLa cells, we observed co-precipitation of active caspase 3 with K18, again demonstrating an interaction between the two proteins. Importantly, this interaction was potentiated by downregulation of eIF3k (Fig. 9E). A similar result was observed in SW13-K8/K18 cells (see Fig. S6 in supplementary material). Together, our findings indicate that endogenous eIF3k interferes with the association of caspase 3 with keratins.

If eIF3k depletion can indeed increase the association of active caspase 3 with keratins, thereby promoting its sequestration in cytoplasmic inclusions, it would lead to an inhibition of the cleavage of caspase substrates that are not present in these inclusions. We therefore tested the processing of ICAD and PARP, which are known to distribute in cytosol and nucleus, respectively. After UV irradiation, we observed that the cleavage of ICAD, evidenced by the disappearance of full-length protein, was diminished in SW13-K8/K18 cells expressing *eIF3k* siRNA, compared with the same cells carrying control siRNA (Fig. 10A, upper panel). Downregulation of eIF3k in parental SW13 cells, however, did not affect ICAD cleavage (Fig. 10A, lower panel). Similarly, eIF3k depletion led to a reduced cleavage of PARP in SW13-K8/K18 cells, but not in SW13 cells (Fig. 10A). In contrast to these cytosolic and nuclear substrates, K18 cleavage by caspase 3 was not affected by eIF3k downregulation, as monitored by the antibody M30 (Fig. 10A, upper panel). In conclusion, our data suggest a role of eIF3k in relieving the caspase-sequestration function of K8/K18, thereby increasing the availability of active caspase 3 to its non-keratin-residing substrates.

Discussion

Here, we identify a previously unrecognized function and subcellular localization of eIF3k. We found that eIF3k colocalizes with K8/K18 filaments in non-apoptotic cells and with K8/K18-containing inclusions in apoptotic cells. Furthermore, using two model cell systems, we demonstrated that endogenous eIF3k sensitizes epithelial cells to both mitochondrial- and death-receptor-mediated apoptosis through a K8/K18-dependent manner. Interestingly, eIF3k does not seem to affect activation of caspase 3. Rather, it promotes the release of active caspase 3 from insoluble, keratin-containing inclusions, thereby increasing availability of this protein to substrates located in subcellular compartments other than the insoluble inclusions (see model in Fig. 10B). Previous studies have revealed that procaspase 3 is concentrated and then activated on keratin fibrils at an early stage of apoptosis; here, it facilitates the cleavage of K18, the disintegration of K8/K18 filaments and the formation of insoluble proteinous inclusions, which trap active caspase 3 and other pro-apoptotic proteins (Lee et al., 2002; Dinsdale

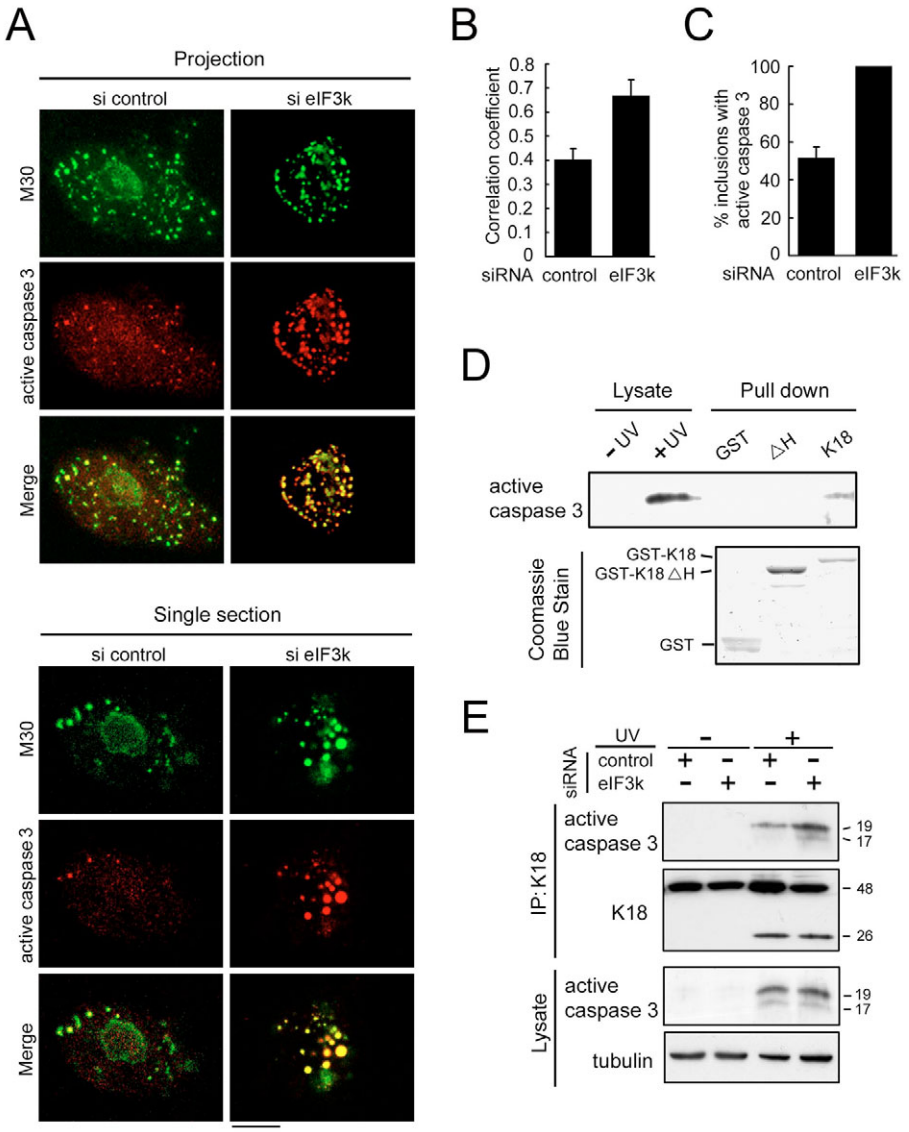

Fig. 9. Downregulation of eIF3k promotes the sequestration of active caspase 3 in K8/K18-residing cytoplasmic inclusions. (A) HeLa cells stably expressing *eIF3k*-specific siRNA (si eIF3k) or control siRNA (si control) as described in Fig. 5 were irradiated with UV and then cultivated for 7 hours. Cells were fixed, double stained with antibody to active caspase 3 and M30 antibody, and examined by confocal microscopy. (Top) The projection view of stacked confocal images, which were created using 19 (for control-siRNA-expressing cells) or 20 (for *eIF3k*-siRNA-expressing cells) overlaying 0.42-μm *z*-sections is shown (see Movies 1, 2 in supplementary material for 3D-reconstructed images). (Bottom) The images of a single *z*-section are shown. Scale bar: 5 μm. (B) Measurement of the correlation coefficient of the M30 (green) and active caspase 3 (red) images shown in A. Confocal images from one section were used for colocalization analysis with the LSM510 software. A total of 14 randomly selected cells in each group were analyzed. (C) Measurement of the percentage of M30-positive dots in a cell with active-caspase-3 signal. M30 dots with a diameter greater than 0.2 μm were counted and the projection view of 3D images from ten randomly selected cells in each group was analyzed. Data shown are mean ± s.d. (D) Interaction of active caspase 3 with K18. HeLa cells irradiated with UV at 0.015 J/cm^2 were lysed for pull-down analysis with GST, GST-K18 (K18), and GST-K18 head-domain deletion mutant (ΔH). Bound proteins and lysates of HeLa cells with or without UV irradiation were analyzed by western blot with antibody to active caspase 3. The relative amounts of various GST fusion proteins used for pull-down analysis are shown on the bottom panel. (E) Downregulation of eIF3k increases the association of active caspase 3 with K18. HeLa cells expressing *eIF3k* siRNA or control siRNA were irradiated with UV at 0.015 J/cm^2 and then cultivated for 12 hours. Cells were lysed with Empigen lysis buffer and lysates were used for immunoprecipitation with anti-K18 antibody. The immunoprecipitates and cell lysates were resolved by SDS-PAGE and then analyzed by western blot with antibodies as indicated. The positions of the19 kDa and 17 kDa fragments of the active caspase 3 as well as the full-length protein (48 kDa) and caspase-3-cleaved K18 (26 kDa) are indicated.

et al., 2004). In this study, we found that the K8/K18-residing eIF3k promotes the release of a portion of active caspase 3 into the cytosol to facilitate the execution of apoptosis in epithelial cells. This regulation of caspase compartmentalization might contribute, at least in part, to the apoptosis-potentiating function of eIF3k, because eIF3k is incapable of affecting apoptosis in epithelial cells lacking keratin proteins. The detailed mechanism by which eIF3k releases keratin-trapped caspase 3 is not completely understood. Because eIF3k inhibits the association of active caspase 3 with keratins, the keratin-interacting eIF3k might compete with this caspase for binding to keratins. In line with this notion, we showed that the head domain of K18 is required for binding both eIF3k and active caspase 3. However, because the stoichiometry of the binding of caspase 3 to K18 is low, their interaction might be indirect. Nevertheless, our study suggests that eIF3k competes directly or indirectly with active caspase 3 for keratin binding and therefore promotes the release of this caspase to the cytosol (Fig. 10B).

The localization of eIF3k in K8/K18-containing inclusions and its function in promoting apoptosis resemble a pro-apoptotic protein, DEDD (Lee et al., 2002). However, DEDD and eIF3k regulate apoptosis through distinct mechanisms. Whereas DEDD concentrates procaspase 3 on the keratin network to promote procaspase 3 activation, which is required for K18 cleavage and filament disruption, eIF3k acts in the subsequent step to facilitate the release of active caspase 3 from insoluble K8/K18-containing inclusions, thereby increasing the availability of caspase 3 to other substrates. This ordered and coordinated action of DEDD and eIF3k on caspase 3 compartmentalization would ensure the cleavage of caspase 3 substrates residing on keratins (including keratins themselves) and in other subcellular structures, and is consistent with the finding that K18 cleavage is a very early event in the apoptosis cascade, preceding loss of membrane asymmetry and DNA fragmentation (Leers et al., 1999). Thus, the K8/K18 network together with its associated proteins, such as DEDD and eIF3k, controls not only the caspase-activation cascade but also caspase

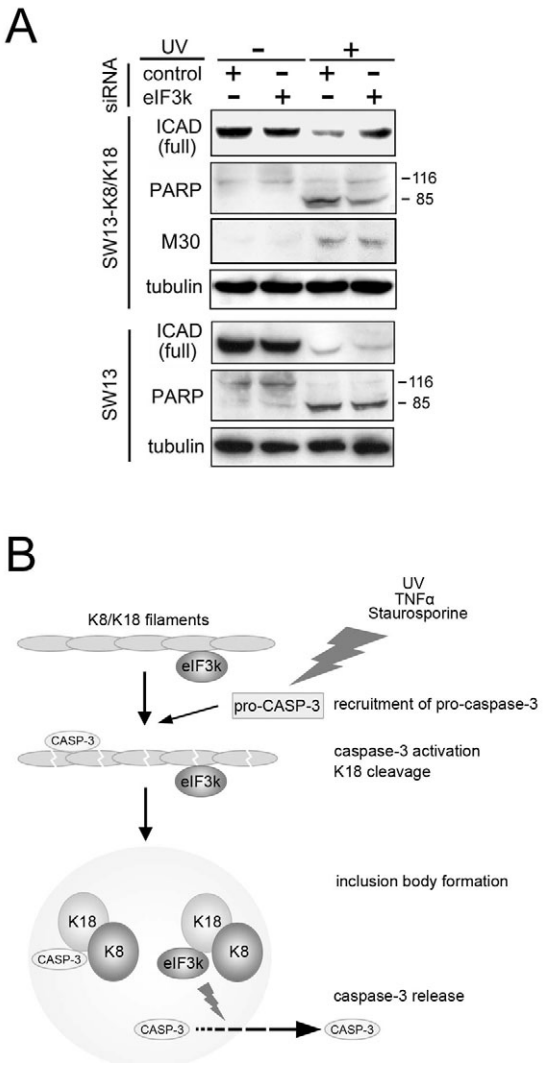

Fig. 10. The effect of eIF3k on the cleavage of caspase 3 nuclear and cytosolic substrates. (A) Downregulation of eIF3k diminishes the cleavage of ICAD and PARP. SW13 or SW13-K8/K18 cells expressing *eIF3k* siRNA or control siRNA were irradiated with UV at 0.015 J/cm^2 and then cultivated for 6 hours (for SW13 cells) or 7 hours (for SW13-K8/K18 cells). Cells were then lysed for western blot analyses with antibodies as indicated. The positions of full-length (116 kDa) and truncated (85 kDa) PARP are indicated. The bands shown in the ICAD blot represent full-length ICAD. (B) Model of eIF3k function during apoptosis. eIF3k is associated with K8/K18 filaments in non-apoptotic cells. Upon induction of apoptosis, procaspase 3 is concentrated in the K8/K18 network (Lee et al., 2002). This leads to a local activation of caspase 3, which in turn cleaves K18. After disintegration of the keratin filaments, cytoplasmic inclusion bodies are formed, which sequester K8, K18, eIF3k and several apoptotic-promoting factors (omitted). In this study, we show that eIF3k inhibits the association of active caspase 3 with K18 and therefore releases this caspase to the cytosol.

compartmentalization, thereby facilitating the proper progression of apoptotic processes in simple epithelial cells.

Our demonstration that eIF3k can sensitize epithelial cells to both death-receptor- and stress-induced apoptosis indicates a general role of eIF3k in apoptosis regulation in epithelial cells. Consistently, eIF3k was found to affect the intracellular distributions of active caspase 3, the common target of both intrinsic and extrinsic pathways. However, these findings do not exclude the possibility that eIF3k affects the distributions of other pro-apoptotic proteins that are sequestered in the keratin-residing cytoplasmic aggregates, such as caspase 9 and TRADD. Notably, the recruitment of TRADD to keratins was reported to contribute to the protective effects of K8/K18 (Inada et al., 2001) and K17 (Tong and Coulombe, 2006) on TNFα-induced apoptosis. It would be interesting to determine whether eIF3k releases keratin-trapped TRADD during TNFα-induced apoptosis.

The apoptosis-regulating function of eIF3k was demonstrated exclusively by the RNA-interference approach, and overexpression of eIF3k in HeLa cells failed to render cells more apoptosis-prone in response to a number of death stimuli (data not shown). This raises a concern that our findings might result from siRNA off-target effects, although the ability of *eIF3k* siRNA to reduce apoptosis can be completely reversed by an siRNA-resistant *eIF3k* construct. Alternatively, the inability of eIF3k overexpression to promote apoptosis suggests that eIF3k is insufficient to elicit a pro-apoptotic function by itself. Notably, immunofluorescence analysis revealed that overexpressed eIF3k displayed a more diffused pattern than the endogenous protein, being only partially colocalized with K18 (compare Fig. 2 with Fig. S7A in supplementary material). This might be due to the amount of eIF3k exceeding the capacity of K18 to bind this protein. In line with this notion, a significantly lower percentage of overexpressed eIF3k was found in the detergent-insoluble fraction, compared with the endogenous protein (Fig. S7B in supplementary material).

The existence of eIF3k both in eIF3 complexes and in keratin filaments raises the issue of whether and how dynamic exchange of eIF3k between these two pools occurs. Intriguingly, a mass-spectrometry-based structural study indicates that eIF3k is among the most easily dissociated subunits and is thus likely to be present on the periphery of eIF3 complexes (Damoc et al., 2007). Currently, the function of eIF3k in translational initiation remains elusive. Our analysis of a *Caenorhabditis elegans eIF3k*-null mutant revealed a dispensable role of this gene in viability (data not shown), suggesting that eIF3k, in analogy with many non-core subunits of the eIF3 complex, is not essential for general translational initiation. Accordingly, a recent study demonstrated that eIF3k is not required for the formation of active eIF3 complex in vitro (Masutani et al., 2007). Notably, several non-core subunits can still elicit function related to translation either by influencing the translational initiation of a subset of mRNA or by stabilizing the architecture of the eIF3 complex (Chang and Schwechheimer, 2004; Zhou et al., 2005). Given the ubiquitous expression of eIF3k and its existence in *Drosophila*, an organism without intermediate filaments, it would be conceivable that eIF3k is involved in a cellular process generally occurring in various cell types and organisms, such as translational initiation. Thus, future studies will be aimed at determining eIF3k function in translational initiation.

Materials and Methods

Cloning of *eIF3k* and generation of antiserum to eIF3k

The cDNA of *eIF3k* was cloned by PCR amplification from a human placenta cDNA library (Clontech). The resulting cDNA fragment was inserted into pGEX-4T. Expression of GST-eIF3k in the bacteria strain BL21 was performed as described previously (Tsai et al., 2000). The GST fusion protein was purified by glutathione Sepharose beads according to the manufacturer's procedures (Amersham Pharmacia) and then used to immunize rabbit for generating anti-eIF3k antiserum.

Plasmid construction

The cDNA fragment of *eIF3k* was inserted into pRK5F to generate mammalian expression plasmids for C-terminally FLAG-tagged eIF3k. pDR2-K8 and pDR2-K18 were described previously (Inada et al., 2001). To knockdown *eIF3k*, an oligonucleotide duplex corresponding to *eIF3k* sequence $_{169}$AACCCAGCCTTCTTT-

$CAGACC_{189}$ was cloned to pSilencer 1.0-U6. An oligonucleotide duplex unrelated to any known genes was also cloned to pSilencer 1.0-U6 to generate the control siRNA construct. To generate the siRNA-resistant *eIF3k* expression construct, site-directed mutagenesis was performed to introduce four silent mutations at positions 174, 177, 180 and 183. The sequences of all constructs were confirmed by DNA-sequencing analysis.

Cell culture and transfection

HeLa and HaCaT cells were maintained in Dulbecco's modified Eagle's medium (DMEM) supplemented with L-glutamine and 10% fetal calf serum. EBNA-SW13 cells were maintained in the same culture medium containing 200 μg/ml G418, whereas SW13-K8/K18 cells were cultured in the EBNA-SW13 medium supplemented with 200 μg/ml hygromycin. Stable transfectants expressing siRNA were maintained in their original culture medium supplemented with 200 μg/ml G418 (for HeLa derivatives) or 1 μg/ml puromycin (for SW13 derivatives). Transient transfection of HeLa cells was performed by the calcium-phosphate method and SW13 cells by the Lipofectamine-2000 reagent.

Apoptosis induction and assay

Apoptosis induction was performed with the following conditions: 1 μM staurosporine for various durations, 2.5 μg/ml Actinomycin D plus 10 ng/ml TNFα for various durations, or UV irradiation at 0.015 or 0.02 J/cm^2 and then cultivated for various durations after irradiation. For analyzing apoptotic cells, cells were fixed in 70% ethanol/30% phosphate buffered saline (PBS) overnight at 4°C, and then incubated in PBS containing 100 μg/ml RNaseA and 50 μg/ml propidium iodide at room temperature for 30 minutes. The cells were analyzed by a FACScalibur cytometer (Becton Dickinson) and cell cycle profiles were analyzed using the CellQuest software.

To determine the clonogenic survival, 1.5×10^3 cells were seeded on a 60 mm plate and then irradiated with low doses of UV (7.5 and 10 J/m^2). Cells were cultured for 8 days and then stained with crystal violet.

Western blot and antibodies

For western blot analysis, cells were lysed in RIPA buffer containing 0.2 M Tris (pH 7.5), 1.5 M NaCl, 10% NP-40, 1% SDS, 10% sodium deoxycholate and protease inhibitors. Lysates containing an equal amount of proteins were subjected to western blot analysis with one of the following antibodies: anti-eIF3k (described above), anti-K8 (M20, Sigma), anti-K18 (CK5, Sigma), anti-FLAG (Santa Cruz Biotechnology), anti-caspase-3 (8G10, Cell Signaling), anti-ICAD (FL-331, Santa Cruz) and anti-PARP (Roche).

Immunofluorescence and confocal studies

Cells grown on coverslides were fixed and permeabilized with 100% cold methanol for 5 minutes at –20°C. The slides were washed three times with PBS and incubated for overnight in blocking solution (PBS containing 10% goat serum, 1% BSA and 0.05% NaN_3). The slides were then incubated for 2 hours at room temperature with one or two of the following antibodies: anti-eIF3k, anti-K8 (M20, Sigma) or anti-K18 (CK5, Sigma). After washing with PBS containing 0.1% Tween-20 (PBST), slides were incubated with FITC-, Texas-Red-, or Cy5-conjugated secondary antibodies together with or without 100 ng/ml Hoechst 33258 for 1 hour at room temperature. The slides were then washed with PBST, mounted and analyzed with a Leica DM RA epifluorescence microscope with a 40× objective lens or a Carl Zeiss LSM510 confocal laser-scanning microscope with a 63× or 100× objective lens. Fluorescent images were captured using the MetaMorph Image System or LSM510 software.

To check the relative localizations of active caspase 3 and inclusion bodies, cells were fixed and double stained with anti-active-caspase-3 (BD Pharmingen) and M30 (Roche) using procedures as described above. The slides were analyzed with a Carl Zeiss LSM510 confocal laser-scanning microscope with a 100× objective lens. The confocal images from serial sections were collected and stacked to generate the 3D image using the LSM510 software.

To examine the colocalization of eIF3k and K8 in tissues, mouse stomach, intestine and prostate were excised, embedded in OCT and frozen in liquid nitrogen. Sections (10 μm) were fixed with acetone at –20°C and then co-stained by anti-eIF3k antibody and anti-K8 antibody (Troma-1, from Hybridoma Center, University of Iowa).

Yeast two-hybrid assay

Yeast two-hybrid assay was performed as described previously (Chen et al., 2005). Briefly, yeast strain L40 was co-transformed with pACT2- and pBTM116-based constructs. The transformants were selected by medium lacking tryptophan, uracil, lysine and leucine (+His). Colonies were transferred to plates containing medium lacking tryptophan, histidine, uracil, lysine and leucine (–His) but supplemented with 20 mM 3-aminotriazole and incubated at 30°C for 6 days to test the expression of the His3 reporter. The same colonies were assayed for β-galactosidase activity.

Immunoprecipitations

HeLa cells were lysed with 2% Empigen BB lysis buffer as described previously (Lowthert et al., 1995), supplemented with 1 mM PMSF, 10 μg/ml aprotinin and 10 μg/ml leupeptin. Cell lysates with an equal amount of proteins were pre-cleared by incubating with protein A or protein G beads for 1 hour at 4°C. The pre-cleared lysates were incubated with anti-eIF3k, anti-K8 or anti-K18 antibody at 4°C for 2 hours, followed by addition of protein A or protein G beads and incubated overnight at 4°C. The beads were washed four times with lysis buffer and resuspended in the SDS sample buffer.

Metabolic labeling and cell proliferation assay

For metabolic labeling, 1.5×10^6 cells were seeded on 35 mm plates in triplicates and the cells were incubated overnight followed by washing twice with serum-free and methionine/cysteine-free medium (Invitrogen). To deplete intracellular pools of sulfur-containing amino acids, the cells were further incubated for 30 minutes at 37°C in methionine/cysteine-free medium. Then, the cells were pulse labeled by incubation for 2 hours with 300 μCi L-[^{35}S]-methionine/cysteine (Pro-Mix; 14.3 mCi/ml; Amersham). The cells were lysed and an aliquot of lysates was resolved by SDS-PAGE. The radioactivity of each lane was determined by scintillation counting. To determine cell proliferation rate, the BrdU ELISA assay was performed according to the manufacturer's instructions (Calbiochem).

Detergent extraction for separating soluble and insoluble proteins

Subconfluent HeLa cells, SW13 cells or their derivatives grown on 35 mm plates were washed once with PBS and then with MES buffer [50 mM MES (pH 6.8), 2.5 mM EGTA and 2.5 mM $MgCl_2$]. The cells were extracted for 5 minutes with 200 μl MES buffer supplemented with 0.5% Triton X-100, 1 mM PMSF, 1 μg/ml aprotinin and 1 μg/ml leupeptin. The supernatant was pre-cleared by centrifugation at 16,000 ***g*** for 10 minutes at 4°C and then was added to 100 μl of 3× SDS sample buffer (soluble fraction). The pellet, together with the detergent-insoluble matrix remaining on the plate, was extracted with 100 μl of 3× SDS sample buffer and then supplemented with 200 μl of MES buffer (insoluble fraction). Equal volumes of the soluble and insoluble fractions were loaded on SDS-PAGE for western blot analysis.

Calculation of the percentage of eIF3k associated with K18 in vivo

Assuming that interaction between eIF3k and K18 is 100% preserved during detergent-extraction and immunoprecipitation processes, the percentage of eIF3k bound to K18 in vivo can be calculated using the following equation:

$$\%\ \text{K18-bound eIF3k} = A/(B\times C)\ ,$$

where A is the % of eIF3k recovered from the anti-K18 immunoprecipitate, B is the % of K18 recovered from the anti-K18 immunoprecipitate (IP efficiency and recovery rate) and C is the % of K18 solubilized by Empigen lysis buffer.

In the experiment shown in supplementary material Fig. S2,

$$A = (72.1/75)/(106.8/0.75) = 0.675\%$$

$$B = (18.8/5)/(24.5/0.5) = 7.67\%$$

$$C = (24.5/0.5)/(24.5/0.5+60/2.5) = 67.1\%\ .$$

Thus,

$$\%\ \text{K18-bound eIF3k} = 0.675\%/(7.67\%\times67.1\%) = 13.1\%\ .$$

We are grateful to Michael Hesse for K8 and K18 constructs, Chin-Chun Hung for confocal analysis and the Pathology Core Facility at IBMS, Academia Sinica for preparation of mouse tissue sections. This study was supported by National Science Council Frontier Grant NSC96-2321-B-001-016.

References

Betz, R. C., Planko, L., Eigelshoven, S., Hanneken, S., Pasternack, S. M., Bussow, H., Van Den Bogaert, K., Wenzel, J., Braun-Falco, M., Rutten, A. et al. (2006). Loss-of-function mutations in the keratin 5 gene lead to Dowling-Degos disease. *Am. J. Hum. Genet.* **78**, 510-519.

Browning, K. S., Gallie, D. R., Hershey, J. W., Hinnebusch, A. G., Maitra, U., Merrick, W. C. and Norbury, C. (2001). Unified nomenclature for the subunits of eukaryotic initiation factor 3. *Trends Biochem. Sci.* **26**, 284.

Burks, E. A., Bezerra, P. P., Le, H., Gallie, D. R. and Browning, K. S. (2001). Plant initiation factor 3 subunit composition resembles mammalian initiation factor 3 and has a novel subunit. *J. Biol. Chem.* **276**, 2122-2131.

Caulin, C., Ware, C. F., Magin, T. M. and Oshima, R. G. (2000). Keratin-dependent, epithelial resistance to tumor necrosis factor-induced apoptosis. *J. Cell Biol.* **149**, 17-22.

Chang, E. C. and Schwechheimer, C. (2004). ZOMES III: the interface between signalling and proteolysis. Meeting on The COP9 Signalosome, Proteasome and eIF3. *EMBO Rep.* **5**, 1041-1045.

Chen, C. H., Wang, W. J., Kuo, J. C., Tsai, H. C., Lin, J. R., Chang, Z. F. and Chen, R. H. (2005). Bidirectional signals transduced by DAPK-ERK interaction promote the apoptotic effect of DAPK. *EMBO J.* **24**, 294-304.

Coulombe, P. A. and Omary, M. B. (2002). 'Hard' and 'soft' principles defining the structure, function and regulation of keratin intermediate filaments. *Curr. Opin. Cell Biol.* **14**, 110-122.

Damoc, E., Fraser, C., Zhou, M., Videler, H., Mayeur, G., Hershey, J., Doudna, J., Robinson, C. and Leary, J. (2007). Strucutral characterization of the human eukaryotic initiation factor 3 protein complex by mass spectrometry. *Mol. Cell. Proteomics* **6**, 1135-1146.

De Martelaere, K., Lintermans, B., Haegeman, G. and Vanhoenacker, P. (2007). Novel interaction between the human 5-HT(7) receptor isoforms. and PLAC-24/eIF3k. *Cell. Signal*. **19**, 278-288.

Dinsdale, D., Lee, J. C., Dewson, G., Cohen, G. M. and Peter, M. E. (2004). Intermediate filaments control the intracellular distribution of caspases during apoptosis. *Am. J. Pathol.* **164**, 395-407.

Gilbert, S., Loranger, A., Daigle, N. and Marceau, N. (2001). Simple epithelium keratins 8 and 18 provide resistance to Fas-mediated apoptosis. The protection occurs through a receptor-targeting modulation. *J. Cell Biol.* **154**, 763-773.

Hedberg, K. K. and Chen, L. B. (1986). Absence of intermediate filaments in a human adrenal cortex carcinoma-derived cell line. *Exp. Cell Res.* **163**, 509-517.

Hinnebusch, A. G. (2006). eIF3: a versatile scaffold for translation initiation complexes. *Trends Biochem. Sci.* **31**, 553-562.

Inada, H., Izawa, I., Nishizawa, M., Fujita, E., Kiyono, T., Takahashi, T., Momoi, T. and Inagaki, M. (2001). Keratin attenuates tumor necrosis factor-induced cytotoxicity through association with TRADD. *J. Cell Biol.* **155**, 415-426.

Kim, S. and Coulombe, P. A. (2007). Intermediate filament scaffolds fulfill mechanical, organizational, and signaling functions in the cytoplasm. *Genes Dev.* **21**, 1581-1597.

Ku, N. O. and Omary, M. B. (1997). Phosphorylation of human keratin 8 in vivo at conserved head domain serine 23 and at epidermal growth factor-stimulated tail domain serine 431. *J. Biol. Chem.* **272**, 7556-7564.

Ku, N. O. and Omary, M. B. (2006). A disease- and phosphorylation-related nonmechanical function for keratin 8. *J. Cell Biol*. **174**, 115-125.

Ku, N. O., Liao, J. and Omary, M. B. (1997). Apoptosis generates stable fragments of human type I keratins. *J. Biol. Chem.* **272**, 33197-33203.

Lee, J. C., Schickling, O., Stegh, A. H., Oshima, R. G., Dinsdale, D., Cohen, G. M. and Peter, M. E. (2002). DEDD regulates degradation of intermediate filaments during apoptosis. *J. Cell Biol.* **158**, 1051-1066.

Leers, M. P., Kolgen, W., Bjorklund, V., Bergman, T., Tribbick, G., Persson, B., Bjorklund, P., Ramaekers, F. C., Bjorklund, B., Nap, M. et al. (1999). Immunocytochemical detection and mapping of a cytokeratin 18 neo-epitope exposed during early apoptosis. *J. Pathol.* **187**, 567-572.

Lowthert, L. A., Ku, N. O., Liao, J., Coulombe, P. A. and Omary, M. B. (1995). Empigen BB: a useful detergent for solubilization and biochemical analysis of keratins. *Biochem. Biophys. Res. Commun.* **206**, 370-379.

Magin, T. M., Vijayaraj, P. and Leube, R. E. (2007). Structural and regulatory functions of keratins. *Exp. Cell Res.* **313**, 2021-2032.

Masutani, M., Sonenberg, N., Yokoyama, S. and Imataka, H. (2007). Reconstitution reveals the functional core of mammalian eIF3. *EMBO J.* **26**, 3373-3383.

Mayeur, G. L., Fraser, C. S., Peiretti, F., Block, K. L. and Hershey, J. W. (2003). Characterization of eIF3k: a newly discovered subunit of mammalian translation initiation factor eIF3. *Eur. J. Biochem.* **270**, 4133-4139.

Oshima, R. G. (2002). Apoptosis and keratin intermediate filaments. *Cell Death Differ.* **9**, 486-492.

Phan, L., Zhang, X., Asano, K., Anderson, J., Vornlocher, H. P., Greenberg, J. R., Qin, J. and Hinnebusch, A. G. (1998). Identification of a translation initiation factor 3 (eIF3) core complex, conserved in yeast and mammals, that interacts with eIF5. *Mol. Cell. Biol.* **18**, 4935-4946.

Porter, R. M. and Lane, E. B. (2003). Phenotypes, genotypes and their contribution to understanding keratin function. *Trends Genet.* **19**, 278-285.

Schutte, B., Henfling, M., Kolgen, W., Bouman, M., Meex, S., Leers, M. P., Nap, M., Bjorklund, V., Bjorklund, P., Bjorklund, B. et al. (2004). Keratin 8/18 breakdown and reorganization during apoptosis. *Exp. Cell Res.* **297**, 11-26.

Schutte, B., Henfling, M. and Ramaekers, F. C. (2006). DEDD association with cytokeratin filaments correlates with sensitivity to apoptosis. *Apoptosis* **11**, 1561-1572.

Shen, X., Yang, Y., Liu, W., Sun, M., Jiang, J., Zong, H. and Gu, J. (2004). Identification of the p28 subunit of eukaryotic initiation factor 3(eIF3k) as a new interaction partner of cyclin D3. *FEBS Lett.* **573**, 139-146.

Toivola, D. M., Tao, G. Z., Habtezion, A., Liao, J. and Omary, M. B. (2005). Cellular integrity plus: organelle-related and protein-targeting functions of intermediate filaments. *Trends Cell Biol.* **15**, 608-617.

Tong, X. and Coulombe, P. A. (2006). Keratin 17 modulates hair follicle cycling in a TNFalpha-dependent fashion. *Genes Dev.* **20**, 1353-1364.

Tsai, Y. T., Su, Y. H., Fang, S. S., Huang, T. N., Qiu, Y., Jou, Y. S., Shih, H. M., Kung, H. J. and Chen, R. H. (2000). Etk, a Btk family tyrosine kinase, mediates cellular transformation by linking Src to STAT3 activation. *Mol. Cell. Biol.* **20**, 2043-2054.

Wei, Z., Zhang, P., Zhou, Z., Cheng, Z., Wan, M. and Gong, W. (2004). Crystal structure of human eIF3k, the first structure of eIF3 subunits. *J. Biol. Chem.* **279**, 34983-34990.

Zhou, C., Arslan, F., Wee, S., Krishnan, S., Ivanov, A. R., Oliva, A., Leatherwood, J. and Wolf, D. A. (2005). PCI proteins eIF3e and eIF3m define distinct translation initiation factor 3 complexes. *BMC Biol.* **3**, 14.

Journal of Cell Science